

Sidebands to the lower kilohertz QPO in 4U 1636–53

P.G. Jonker^{1,2*}, M. Méndez^{2,3}, M. van der Klis⁴

¹*Harvard–Smithsonian Center for Astrophysics, 60 Garden Street, Cambridge, MA 02138, Massachusetts, U.S.A.*

²*SRON, National Institute for Space Research, Sorbonnelaan 2, 3584 CA, Utrecht, The Netherlands*

³*Astronomical Institute, Utrecht University, P.O. Box 80000, 3508 TA, Utrecht, The Netherlands*

⁴*Astronomical Institute “Anton Pannekoek”, University of Amsterdam, Kruislaan 403, 1098 SJ Amsterdam, The Netherlands*

1 November 2018

ABSTRACT

In this Paper we report on further observations of the third and fourth kilohertz quasi-periodic oscillations (QPOs) in the power spectrum of the low-mass X-ray binary (LMXB) 4U 1636–53. These kilohertz QPOs are sidebands to the lower kilohertz QPO. The upper sideband has a frequency 55.5 ± 1.7 Hz larger than that of the contemporaneously measured lower kilohertz QPO. Such a sideband has now been measured at a significance $> 6\sigma$ in the power spectra of three neutron star LMXBs (4U 1636–53, 4U 1728–34, and 4U 1608–52). We also confirm the presence of a sideband at a frequency ~ 55 Hz less than the frequency of the lower kilohertz QPO. The lower sideband is detected at a 3.5σ level, only when the lower kilohertz QPO frequency is between 800 and 850 Hz. In that frequency interval the sidebands are consistent with being symmetric around the lower kHz QPO frequency. The upper limit to the rms amplitude of the lower sideband is significant lower than that of the upper sideband for lower kilohertz QPO frequencies > 850 Hz. Symmetric sidebands are unique to 4U 1636–53. This might be explained by the fact that lower kilohertz QPO frequencies as high as 800–850 Hz are rare for 4U 1728–34 and 4U 1608–52. Finally, we also measured a low frequency QPO at a frequency of ~ 43 Hz when the lower kilohertz QPO frequency is between 700–850 Hz. A similar low-frequency QPO is present in the power spectra of the other two systems for which a sideband has been observed. We briefly discuss the possibility that the sideband is caused by Lense–Thirring precession.

Key words: stars: individual (4U 1636–53) — accretion: accretion discs — stars: binaries — stars: neutron — X-rays: binaries

1 INTRODUCTION

One of the important discoveries made with the Rossi X-ray Timing Explorer (RXTE) satellite is that of the kilohertz quasi-periodic oscillations (QPOs) in the power spectra of ~ 20 accreting neutron star low-mass X-ray binaries (see van der Klis 2000 for a review). Kilohertz QPOs are caused by the motion of matter in regions of spacetime within a few kilometres of the surface of accreting neutron stars, where strong-field gravity is required to describe such motion. They potentially allow one to detect strong-field effects and to constrain the neutron star mass-radius relation. Although there is as yet no agreement about the precise physical mechanism underlying kilohertz QPOs, most models agree that the frequency of one of the observed kilohertz QPOs reflects the frequency of orbital motion at the inner edge of the accretion disc.

The basic phenomenology of kilohertz QPOs consists of two kilohertz QPO peaks, which are separated by $\Delta\nu=200$ –360 Hz and which move in frequency by up to 700 Hz in general correlation with mass accretion rate indicators (again see van der Klis 2000 for a review). The highest observed frequency is ~ 1330 Hz (van Straaten et al. 2000), corresponding in the case of a $1.4 M_{\odot}$ neutron star to an orbital radius as tight as 15 km. Some of these sources also show X-ray bursts, in which burst oscillations are seen which last for a few seconds and have frequencies between 270 and 620 Hz (see Strohmayer & Bildsten 2004 for a review). These oscillations usually drift by 1–2 Hz but are near the neutron star spin frequency in each source (Chakrabarty et al. 2003). In the millisecond pulsar SAX J1808.4–3658 $\Delta\nu$ has been found to be equal to half the spin frequency, which disproves spin-orbit beat frequency models (Wijnands et al. 2003) and suggests instead that the neutron star spin induces resonances in the disk flow, perhaps involving the

* email : pjonker@cfa.harvard.edu

general relativistic epicyclic frequencies (Abramowicz et al. 2003; Wijnands et al. 2003; Lamb & Miller 2003).

After extensive searches for additional kilohertz QPO peaks at theoretically predicted frequencies which remained unsuccessful (e.g. in Sco X-1; Méndez & van der Klis 2000), Jonker et al. (2000) discovered sidebands at a frequency 50–65 Hz above the lower kilohertz QPO in 4U 1608–52, 4U 1728–34, and 4U 1636–53. Magnetospheric modulation of the lower kilohertz QPO, a beat phenomenon taking place inside the marginally stable orbit as well as Lense-Thirring precession are possible explanations for these sidebands (Jonker et al. 2000). Psaltis (2000) demonstrated that the hydrodynamic disk mode model (Psaltis & Norman 1999) naturally produces a sideband at a frequency near that observed plus several other, as yet unobserved peaks; no other models have so far been able to explicitly accommodate the sideband. The 50–65-Hz frequency difference between the lower kilohertz QPO and the sideband frequency, the ‘sideband separation’ $\Delta\nu_{SB}$, is different in each source and not identical to any of the other QPO frequencies simultaneously observed in the 10–100 Hz frequency range (Jonker et al. 2000).

In this Paper we find evidence for symmetric sidebands to the lower kilohertz QPO in the atoll source 4U 1636–53.

2 OBSERVATIONS, ANALYSIS, AND RESULTS

We used all the proportional counter array (PCA) data from RXTE observations of 4U 1636–53 available to us at the beginning of 2004. Hence, we included the data used by Jonker et al. (2000). The analysis we performed was the same as that done by Jonker et al. (2000). Below, a condensed description of the analysis steps is given; more details can be found in Jonker et al. (2000).

Using 128 s-long segments of high time resolution PCA data (122 μ s resolution), we calculated power spectra up to a Nyquist frequency of 4096 Hz in an energy band of 2–60 keV. The power spectra were searched for lower kilohertz QPOs which are narrow (full-width at half maximum, FWHM, less than ~ 10 Hz) and detected in 128 s at a significance larger than 2σ . This resulted in a selection of 244 ksec of data.

The lower kilohertz QPO was traced using a dynamical power spectrum (e.g. see plate 1 in Berger et al. 1996) to visualise the time evolution of the QPO frequency. For each power spectrum the lower kilohertz QPO peak was fitted in a range of 200 Hz centred on the traced frequency using a function consisting of a constant plus a Lorentzian. This provides us with a lower kilohertz QPO frequency measurement for each 128 s power spectrum. We used the shift-and-add technique described by Méndez et al. (1998) to shift each lower kilohertz QPO to a reference frequency. Next, the shifted, aligned, power spectra were averaged. The average power spectrum was finally fitted in the range 512–2048 Hz so as to exclude the edges which are distorted due to the shifting. The fit function consisted of a constant to fit the noise and three or four Lorentzians representing the QPOs. The fitted average power spectrum is displayed in Figure 1. Errors on the fit parameters were calculated using $\Delta\chi^2 = 1.0$ (1 σ single parameter).

We clearly detected the two kilohertz QPOs and the

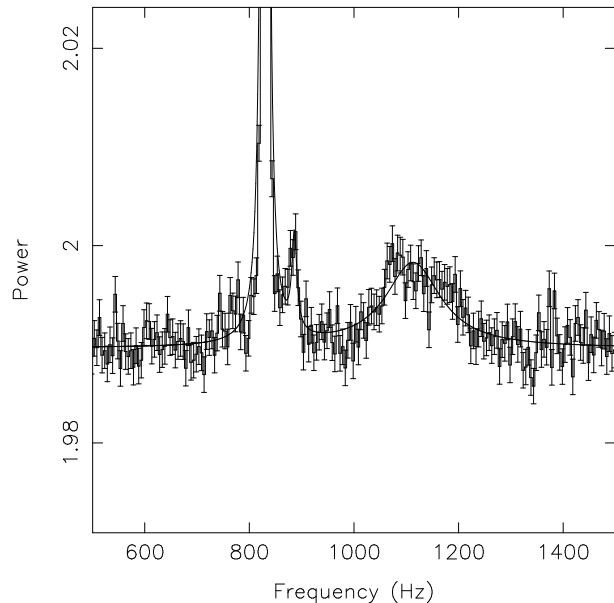


Figure 1. The average power density spectrum of 4U 1636–53 showing the lower kilohertz QPO (the peak is off-scale), the upper kilohertz QPO, and the upper sideband to the lower kilohertz QPO. Due to the shift-and-add method applied in the analysis only the frequency differences are meaningful (see text and references therein). The drawn line represents the best fit of a function consisting of a constant and three Lorentzians. The power in the Y-axis is given in Leahy units.

sideband to the lower kilohertz QPO. The sideband was detected at a significance of 6σ , confirming our previous 3σ detection of the sideband in 4U 1636–53 (Jonker et al. 2000). The frequency difference between the frequency of the lower kilohertz QPO and that of the sideband, $\Delta\nu_{SB} = 55.5 \pm 1.7$ Hz. The average kilohertz QPO frequency separation, $\langle \Delta\nu = \nu_{\text{upper}} - \nu_{\text{lower}} \rangle$, is 283 ± 5 Hz. The FWHM of the sideband, the lower kilohertz QPO and the upper kilohertz QPO is 12.7 ± 2.7 Hz, 4.86 ± 0.04 Hz, and 130 ± 11 Hz, respectively. Due to the fact that we have combined data with either 3, 4, or 5 active proportional counter units (PCUs) we cannot determine the fractional rms amplitude of the QPO peaks from the combined data. Therefore, we selected data where only 3, 4, or 5 PCUs were active, we fitted those data sets separately. In those separate fits we fixed the FWHM and the frequency of the QPOs to the values found using the complete data set. The fractional rms amplitude of the sideband is consistent with what was found before (see Table 1 and Jonker et al. 2000).

In order to search for changes in the sideband separation frequency $\Delta\nu_{SB}$ we averaged shifted power spectra based on the unshifted frequency of the lower kilohertz QPO in three frequency bands; a lower kilohertz QPO frequency between 700–800 Hz, 800–850 Hz, and above 850 Hz. Interestingly, the average power spectrum in the lower kilohertz QPO frequency interval 800–850 Hz showed evidence for two sidebands located symmetrically around the lower kilohertz QPO peak (see Figure 2). The results of fits to these averaged power spectra are given in Table 1.

Adding more data with respect to the analysis performed by Jonker et al. (2000), we now find a QPO at low frequencies (~ 43 Hz, see Figure 3). In order to compare the

Table 1. Properties of the lower and upper kilohertz QPO (ν_1 and ν_2 , respectively), the sidebands to the lower kilohertz QPO, and the low frequency QPO. The properties displayed below the last horizontal line have been determined without using the shift-and-add technique. The FWHM of the lower sideband has in all cases been fixed to that of the upper sideband.

	All frequencies	700–800 Hz	800–850 Hz	850–920 Hz
Amount of data (ksec)	244	64	80	99
Mean $\nu_1 \pm$ stan. dev. (Hz)	830 ± 50	763 ± 25	828 ± 15	877 ± 17
$\Delta\nu$ (Hz)	283 ± 5	325 ± 6	286 ± 9	249 ± 4
$\Delta\nu_{\text{SB,lower}}$ (Hz)	–	–	55.1 ± 2.5	–
$\Delta\nu_{\text{SB,upper}}$ (Hz)	55.5 ± 1.7	47.7 ± 3.5	57.0 ± 2.1	56 ± 2
rms amplitude ν_1 (%)	7.54 ± 0.01	7.94 ± 0.04	7.86 ± 0.02	7.12 ± 0.03
FWHM ν_1	4.86 ± 0.04	5.4 ± 0.1	4.45 ± 0.06	4.90 ± 0.06
rms amplitude ν_2 (%)	4.03 ± 0.11	4.5 ± 0.3	4.0 ± 0.2	3.4 ± 0.2
FWHM ν_2	130 ± 11	104 ± 15	120 ± 18	87 ± 13
rms amplitude $\nu_{\text{SB,lower}}$ (%)	$< 0.9^a$	$< 1.5^a$	1.2 ± 0.2	$< 0.8^a$
rms amplitude $\nu_{\text{SB,upper}}$ (%)	1.3 ± 0.1	1.7 ± 0.2	1.4 ± 0.2	1.2 ± 0.1
FWHM $\nu_{\text{SB,upper}}$	12.7 ± 2.7	14 ± 5	12 ± 4	10 ± 4
rms amplitude ν_{low} (%)	–	2.7 ± 0.2	2.3 ± 0.1	$< 1.6^a$
FWHM ν_{low} (Hz)	–	17 ± 3	20 ± 4	–
Frequency ν_{low} (Hz)	–	42.1 ± 0.8	43.5 ± 1.6	–

^a 95% upper limits (determined using $\Delta\chi^2 = 2.71$).

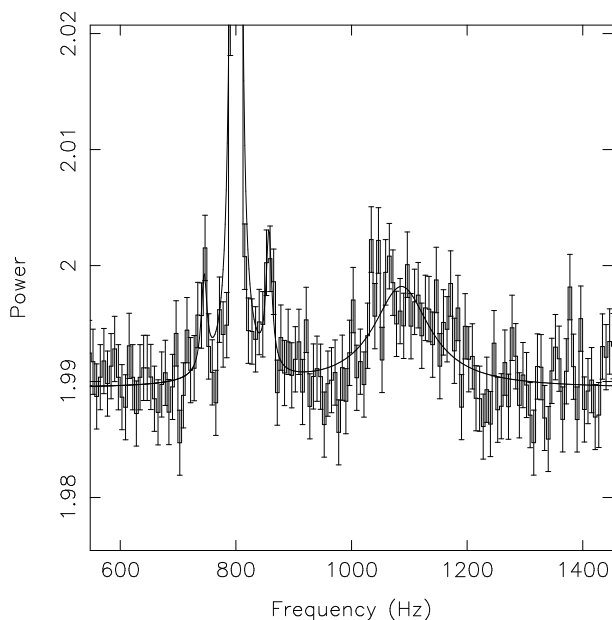


Figure 2. The average power density spectrum of 4U 1636–53 selecting only lower kilohertz QPO frequencies between 800–850 Hz. The two kilohertz QPOs and the sideband on the high frequency side of the lower kilohertz QPO are visible. In addition, a sideband on the low frequency side of the lower kilohertz QPO can be discerned (3.5σ single trial). Due to the shift-and-add method applied in the analysis only the frequency differences are useful (see text and references therein). The drawn line represents the best fit of a function consisting of a constant and four Lorentzians.

properties of this low-frequency QPO with that of the kilohertz QPOs and the kilohertz QPO separation frequencies we fitted the average unshifted power spectrum in the frequency range from 1/16–256 Hz in the three lower kilohertz QPO frequency intervals as shown in Table 1. In the frequency range 850 Hz and above the low frequency QPO was undetectable (see Table 1).

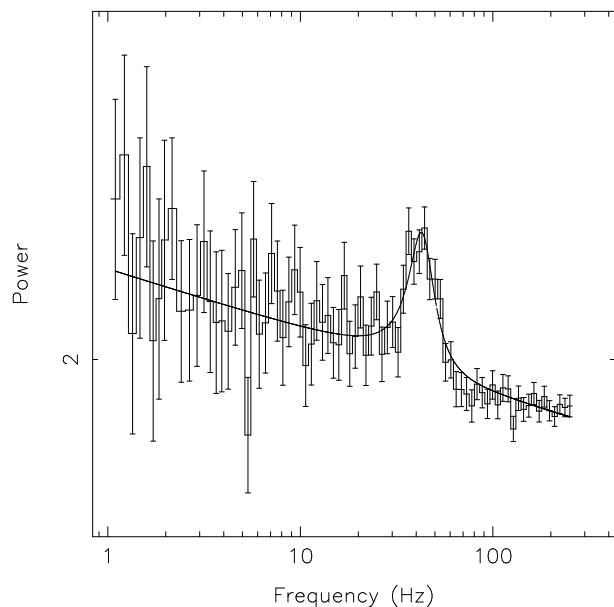


Figure 3. The low frequency part of the average power density spectrum of 4U 1636–53 selecting only lower kilohertz QPO frequencies between 700–850 Hz. A low frequency QPO at a frequency of ~ 43 Hz is visible. The drawn line represents the best fit of a function consisting of a power law to fit the underlying red noise continuum and a Lorentzian to fit the low frequency QPO. We did not apply any shift to produce this power spectrum.

3 DISCUSSION

Following the discovery by Jonker et al. (2000) of a new, third, kilohertz QPO in the power spectra of the three atoll-type low-mass X-ray binaries 4U 1608–52, 4U 1728–34, and 4U 1636–53 we obtained additional data with the RXTE satellite of 4U 1636–53 with the goal to study in detail the properties of this third kilohertz QPO, also known as the sideband to the lower kilohertz QPO. We selected 4U 1636–53 since in that source there is evidence for the presence

of two sidebands located symmetrically around the lower kilohertz QPO peak frequency.

We confirm the presence of a sideband at a frequency 55.5 ± 1.7 Hz higher than that of the lower kilohertz QPO frequency in 4U 1636–53 at a 6σ significance level. Furthermore, the addition of the extra data allowed us to investigate the sideband(s) as a function of the lower kilohertz QPO frequency. We found that when the lower kilohertz QPO has a frequency in the range 800–850 Hz there is significant evidence (3.5σ , single trial) for the presence of a sideband at the lower frequency side of the lower kilohertz QPO. Selecting lower kilohertz QPO frequencies >850 Hz and when combining all the data, the rms amplitude of the lower sideband is significantly less than that of the upper sideband. For the frequency range 700–800 Hz the upper limit is consistent with the rms amplitude of the upper sideband.

In the framework of the sonic–point and spin–resonance model of Lamb & Miller (2003), the sideband is unlikely to be caused by Lense–Thirring precession at the radius where the spin–resonance occurs (near the orbital radius with a Kepler frequency of $\nu_{spin}/2$), since for neutron star spin frequencies such as those considered here, the Lense–Thirring precession frequency at that radius is ≈ 2 Hz, this is much too low. It is possible though that the radiation pattern responsible for the upper kilohertz QPO is modulated by the Lense–Thirring precession at the sonic–point radius, this modulation would then in turn modulate the formation of the lower kilohertz QPO. In such a scenario the upper kilohertz QPO should also display sidebands. The fact that these have not yet been detected can be explained by the large FWHM of the upper kilohertz QPO, which precludes the detection of such sidebands. The skewed shape of the upper kilohertz QPO in the average power spectrum (see e.g. Fig 1) can be explained by the fact that the upper kilohertz QPO rms amplitude and $\Delta\nu$ change as a function of kilohertz QPO frequency (e.g. Méndez et al. 1998, Table 1).

If Lense–Thirring precession is responsible for the production of the sideband, and if the sideband separation frequency $\Delta\nu_{SB}$, reflects the Lense–Thirring precession frequency, $\Delta\nu_{SB}$ would be expected to change as the Keplerian frequency squared ($\Delta\nu_{SB} \propto \nu_K^2$). In Figure 4 we plotted $\Delta\nu_{SB}$ as a function of the lower (*left panel*) and upper kilohertz QPO (*right panel*), respectively. The sideband separation frequency $\Delta\nu_{SB}$ is consistent with being constant when the lower/upper kilohertz QPO frequency changed by $\sim 100/\sim 38$ Hz, respectively. The best fitting quadratic relation that would be appropriate assuming the lower/upper kilohertz QPO reflects the Keplerian motion at a preferred radius in the disc and $\Delta\nu_{SB}$ the Lense–Thirring precession frequency at that same radius is also shown. The normalisation of the quadratic curve is given by $\nu_{LT} = \frac{8\pi^2 I_K^2 \nu_s}{c^2 M_{NS}}$ (ν_{LT} is the Lense–Thirring precession frequency, I the moment of inertia of the neutron star, ν_s the spin frequency of the star which is ~ 581 Hz in case of 4U 1636–53 from Strohmayer et al. 1997, c the speed of light, and M_{NS} the mass of the neutron star). The curve in the left panel requires I_{45}/m to be 3.05 ± 0.07 , that in the right panel 0.17 ± 0.01 , where I_{45} and m are in units of 10^{45} g cm² and M_\odot , respectively; the expected range of this quantity is between 0.5 and 2 (Stella & Vietri 1998).

Recently, a model explaining the kilohertz QPOs

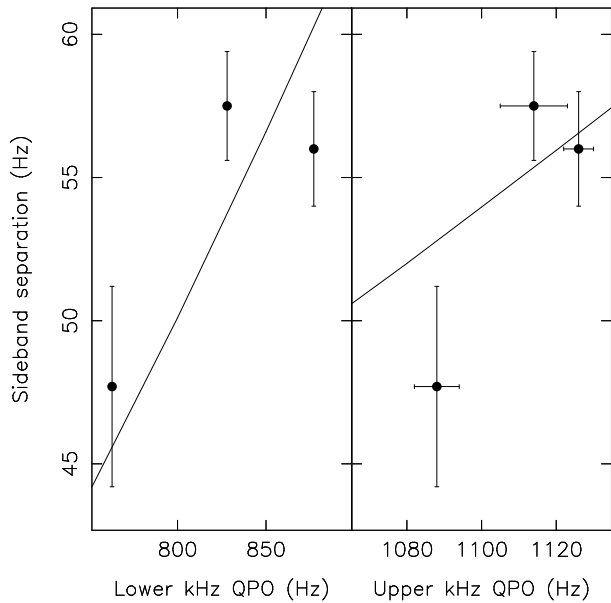


Figure 4. *Left panel:* The sideband separation frequency plotted vs. the lower kilohertz QPO frequency, $\Delta\nu_{SB}$. The full line is the quadratic relation between $\Delta\nu_{SB}$ and the lower kilohertz QPO assuming the lower kilohertz QPO reflects the Keplerian frequency and assuming the sideband is formed due to a modulation caused by Lense–Thirring precession at that radius. *Right panel:* same as the left panel but for the upper kilohertz QPO.

has been proposed that invokes the existence of a non-linear resonance between the vertical and radial epicyclic frequencies in an accretion disc around a neutron star (Abramowicz et al. 2003). Some versions of this model also include a resonance of these frequencies with the spin frequency of the neutron star (Kluźniak et al. 2004; Lee et al. 2004). The resonance model has been introduced as a way to explain the existence of preferred values in the distribution of QPO frequency ratios (Abramowicz et al. 2003; but see Belloni et al. 2004) as well as the commensurability of the neutron star spin and the kilohertz QPO frequency separation. So far it has not been explored whether a resonance mechanism could also explain the sidebands to the kilohertz QPOs. For instance, it may be possible that the Lense–Thirring precession at the radius at which the main resonance between the vertical and radial epicyclic frequencies occurs produces a modulation of the amplitude of the kilohertz QPOs. In principle, this modulation should produce equally strong sidebands, and should also produce sidebands on both QPOs. Alternatively, since for a rotating neutron star the azimuthal (Keplerian) frequency is larger than the vertical frequency, the sideband could be due to a resonance involving the azimuthal frequency at a radius at which a resonance between the vertical and radial epicyclic frequencies produce the upper and lower kilohertz QPOs. For instance, in this scenario a resonance between the azimuthal and radial frequencies would produce a QPO at a frequency slightly higher than that of the upper kilohertz QPO. The advantage of this mechanism compared to an amplitude modulation is that it could in principle explain the fact that the upper sideband is stronger than the lower sideband. However, it remains unclear how a QPO at a fre-

quency ≈ 55 Hz higher than that of the lower kilohertz QPO would appear in this scenario.

Previously, 4U 1636–53 was the only source out of the three sources where a sideband to the lower kilohertz QPO that showed no low-frequency QPO (Jonker et al. 2000). Now, with the additional RXTE data, we could identify a low-frequency QPO at a frequency of ~ 43 Hz, similar to the one found in 4U 1728–34 and 4U 1608–53 (see Jonker et al. 2000). The probable reason why this low-frequency QPO was not observed before is that the source did not sample the states where this QPO is present often. Much of the new data were obtained in the state showing the low-frequency QPO. From Table 1 it can be seen that the lower kilohertz QPO frequency has to be below 850 Hz for the low-frequency QPO to be detected. Comparing the observed frequency distributions of the data set used by Jonker et al. (2000) (Figure 5 shaded area *top panel*) with that used in this work (Figure 5 overall grey line *top panel*) it is clear that besides an increase in the amount of data, the lower kilohertz QPO frequencies in the range 700–850 Hz are much better sampled in the new dataset. A likely explanation for the fact that the distribution of the observed lower kilohertz QPO frequencies is different during the new RXTE observations from that observed in the data set used by Jonker et al. (2000), is that the X-ray flux of 4U 1636–53 has been decreasing over the last few years (see Fig. 5 *bottom panel*), allowing many of the additional new observations to be obtained at flux levels and at lower kilohertz QPO frequencies which were sparsely observed before in 4U 1636–53 with RXTE

ACKNOWLEDGMENTS

Support for this work was provided by NASA through Chandra Postdoctoral Fellowship grant number PF3–40027 awarded by the Chandra X-ray Center, which is operated by the Smithsonian Astrophysical Observatory for NASA under contract NAS8–39073.

REFERENCES

- Abramowicz, M. A., Karas, V., Kluzniak, W., Lee, W. H., Rebusco, P., 2003, PASJ, 55, 467
 Belloni, T., Méndez, M., Homan, J., 2004, submitted to ApJ
 Berger, M., et al., 1996, ApJ, 469, L13
 Chakrabarty, D., Morgan, E. H., Muno, M. P., Galloway, D. K., Wijnands, R., van der Klis, M., Markwardt, C. B., 2003, Nat, 424, 42
 Jonker, P. G., Méndez, M., van der Klis, M., 2000, ApJ, 540, L29
 Kluzniak, W., Abramowicz, M. A., Kato, S., Lee, W. H., Stergioulas, N., 2004, ApJ, 603, L89
 Lamb, F. K., Miller, M. C., 2003, ApJ
 Lee, W. H., Abramowicz, M. A., Kluzniak, W., 2004, ApJ, 603, L93
 Méndez, M., van der Klis, M., 2000, MNRAS, 318, 938
 Méndez, M., van der Klis, M., van Paradijs, J., 1998, ApJ, 506, L117

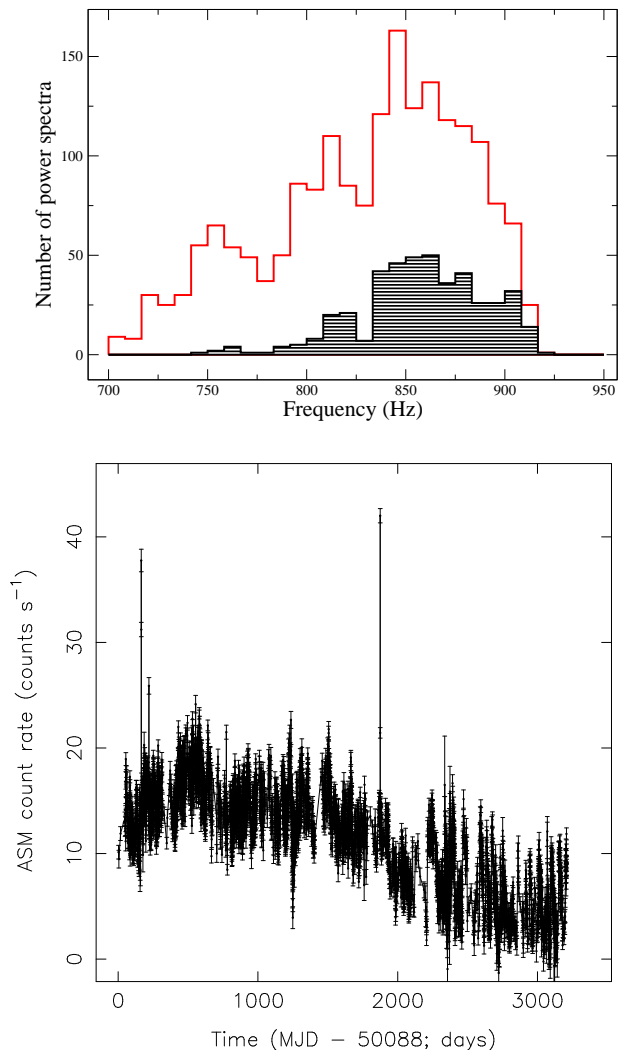


Figure 5. *Top panel:* The distribution of the lower kilohertz QPO frequency for the data used by Jonker et al. (2000; black shaded area) and the data used in this work (grey histogram). Note that the drawn grey distribution includes the black shaded data. It is clear that, besides an increase in data volume, a larger range in lower kilohertz QPO frequency was sampled with the current data. The occurrence of peaks in the frequency distribution can be explained by a random walk in kilohertz QPO frequency (see for instance Belloni et al. 2004). *Bottom panel:* The ASM count rate history of the source 4U 1636–53. A clear decay in overall brightness can be seen starting around MJD ~ 51590 . The strong narrow peaks are caused by the occurrence of superbursts (Wijnands 2001; Strohmayer & Markwardt 2002).

- Méndez, M., van der Klis, M., Wijnands, R., Ford, E. C., van Paradijs, J., Vaughan, B. A., 1998, ApJ, 505, L23
 Psaltis, D., 2000, ApJ, submitted, astro-ph/0010316
 Psaltis, D., Norman, C., 1999, ApJ, submitted, astro-ph/0001391
 Stella, L., Vietri, M., 1998, ApJ, 492, L59
 Strohmayer, T. E., Bildsten, L., 2004, in X-ray binaries, Cambridge Astrophysics Series: Cambridge University Press, 2004, edited by Lewin, W. H. G.; Van der Klis,

6 *Jonker, Méndez, & van der Klis*

- M.
Strohmayer, T. E., Markwardt, C. B., 2002, *ApJ*, 577, 337
Strohmayer, T. E., Jahoda, K., Giles, A. B., Lee, U., 1997,
ApJ, 486, 355
van der Klis, M., 2000, *ARA&A*, 38, 717
van Straaten, S., Ford, E. C., van der Klis, M., Méndez,
M., Kaaret, P., 2000, *ApJ*, 540, 1049
Wijnands, R., 2001, *ApJ*, 554, L59
Wijnands, R., van der Klis, M., Homan, J., Chakrabarty,
D., Markwardt, C. B., Morgan, E. H., 2003, *Nat*, 424, 44